Structure of ^{39}Ar

E. K. Warburton
Brookhaven National Laboratory, Upton, New York 11973
(Received 20 February 1987)

A spherical shell-model calculation of the odd- and even-parity states of ^{39}Ar is made in a full *sdpf* model space. The calculation includes absolute binding energies and energy spectra, single-neutron spectroscopic factors, and electromagnetic and beta decay observables. Agreement with experiment is fairly good. Comparison is hampered by incomplete experimental knowledge and by the presence of low-lying intruder states.

I. INTRODUCTION

^{39}Ar has low-lying odd- and even-parity levels which are expected to arise from ^{16}O$(2s,1d)^{22}(1f,2p)^1$ and ^{16}O$(2s,1d)^{21}(1f,2p)^2$ configurations. Previous shell-model calculations have been performed for the states in model spaces truncated to $d_{3/2}^{-2}f_{7/2}$ (Ref. 1), $d_{3/2}^{-2}(1f_{7/2},2p_{3/2})^1$ (Refs. 2 and 3), and $(2s,1d)^{-2}(1f_{7/2},2p_{3/2})^1$ (Ref. 4). No shell-model calculations have been reported for the even-parity levels.

In the present shell-model study we make use of the recently developed[5] interaction SDPF, which is intended for use in the full

$$^{16}\mathrm{O}(2s_{1/2},1d_{5/2},1d_{3/2})^{A-16-n}(1f_{7/2},2p_{3/2},1f_{5/2},2p_{1/2})^n$$

configuration space. Calculations are carried out for both odd- and even-parity states without truncation within the two major shells which are involved. In addition to energy spectra, the results include calculations for ^{39}Cl$(\beta^-)^{39}$Ar (both allowed and forbidden), one-neutron transfer spectroscopic factors, and electromagnetic decays. The calculations are described in the next section and the results are considered in the following sections.

The experimental results for ^{39}Ar to which we shall compare our calculations are taken mostly from the compilation of Endt and van der Leun.[6] Results for ^{39}Cl$(\beta^-)^{39}$Ar and for some γ-ray branching ratios are from the preceding paper (Ref. 7). The comparison of the shell-model results to experiment is complicated because of indefinite spin-parity assignments and the presence of "intruder" states. This complexity renders the following description less straightforward than is desirable. Nevertheless, an investigation of ^{39}Ar was considered important because it is the first nucleus below possible shell closure at $A\sim 40$ for which we may compare experiment to the predictions of the full SDPF calculation for both one and two nucleons in the (fp) shell. In fact, with the computer resources presently available, it is also the only nucleus in this category for which we may do this.

II. CALCULATIONS

A. The interaction

The SDPF interaction consists of the "universal" $2s,1d$ interaction of Wildenthal,[8,9] a modified van Hees–Glaudemans[10] interaction for the $1f,2p$ shell, and a modified Millener-Kurath interaction for the cross-shell interaction between the $2s,1d$ and $1f,2p$ shells.[11] The modifications to these interactions are described in Refs. 5 and 12. The interaction is considered most suitable for levels in nuclei near $A\sim 40$ with 0—3 active nucleons in the fp shell and the remainder in the sd shell.

Calculations were done with the computer program OXBASH.[13] OXBASH works in the m scheme but utilizes projected basis vectors which have good J and T.

B. Electromagnetic observables

Results for electromagnetic transitions are calculated in the form of matrix elements, $M(\lambda)$, or transition strengths, $B(\lambda)$, for specific multipolarity λ. The relation for a transition $i\rightarrow f$ is

$$(2J_i+1)B(\lambda)=[M(\lambda)]^2\ . \tag{1}$$

The $B(\lambda)$ are the conventional transition strengths (see, e.g., Ref. 14). They are given either in units of $e^2\,\mathrm{fm}^{2L}$ and $\mu_N^2\,\mathrm{fm}^{2L-2}$ for EL and ML, respectively, or in Weisskopf units (W.u.) (Ref. 14). For ^{39}Ar, the $B(\lambda)$ values in $e^2\,\mathrm{fm}^{2L}$ or $\mu_N^2\,\mathrm{fm}^{2L-2}$ corresponding to 1 W.u. are 0.741, 7.857, 90.334, 1.791, and 18.977 for $E1$, $E2$, $E3$, $M1$, and $M2$ transitions, respectively.

Another observable of interest is the mixing ratio of $L+1$ to L radiation in a specific transition. This observable, designated $x(L+1/L)$, has a meaningful sign as well as magnitude. Experimental values are given by Endt and van der Leun[6] using the sign convention of Rose and Brink,[15] and we use this convention for the predictions of $x(L+1/L)$ and for the relative signs of the matrix elements $M(L+1)$ and $M(L)$.

Electromagnetic matrix elements are calculated using harmonic oscillator radial wave functions with the length parameter $b=(41.467/\hbar\omega)^{1/2}$ fm evaluated from $\hbar\omega=45A^{-1/3}-25A^{-2/3}$ MeV. $E1$ and $M2$ electromagnetic matrix elements were calculated with free nucleon operators. $M1$ transitions were calculated with an effective operator derived from a least-squares fit to selected $M1$ transition matrix elements in the $(2s,1d)$ shell. The fit, described recently by Brown,[16] used the USD interaction. $E2$ transitions utilized the effective charges $e_p=1.29e$, $e_n=0.49e$, which also result from a least-squares fit of USD results to $(2s,1d)$ transitions.[16] $E3$ matrix elements use effective charges of $e_p=1.5e$ and $e_n=0.5e$.

C. Beta decay

For allowed Gamow-Teller ($n=0$) or unique first-forbidden decay ($n=1$), comparison to theory is most conveniently made via the transition strength (matrix element squared), which we define as[5]

$$B_n = 6166 \left\{ \frac{[(2n+1)!!]^2}{(2n+1)} \right\} \lambdabar_{Ce}^{2n} (f_n t)^{-1} , \quad (2)$$

where $2\pi\lambdabar_{Ce}$ is the Compton wavelength of the electron ($\lambdabar_{Ce}=386.159$ fm). Equation (2) gives

$$B_0 = 6166/f_0 t , \quad 10^{-6} B_1 = 2758/f_1 t \ \text{fm}^2 , \quad (3)$$

where f_0 and f_1 are the Fermi functions calculated with shape factors of unity and $\sim \frac{1}{12}(p^2+q^2)$, respectively. The nonunique predictions are compared to experiment via the f value defined by $f=(6166/t)$BR (Ref. 17), where BR denotes the B branching ratio. Allowed Gamow-Teller (GT) transitions were calculated with an effective operator[5,16,18] derived similarly to the $M1$ operator and also with the operator appropriate to free nucleons. Calculations of first-forbidden beta decay observables use operators appropriate to free nucleons and either harmonic oscillator or Woods-Saxon radial wave functions. For the present we only quote the results of the first-forbidden calculations; full details are given elsewhere.[19]

D. The reliability of the predictions

A few words about the expected accuracy of our calculations are in order. The calculations done to date[5,12] with the SDPF interaction give level energies with about 250-keV root-mean-square deviation from experiment. We expect to predict medium to strong $M1$, $E2$, and $E3$ transitions and GT β transitions with quite high accuracy (within $\sim 50\%$ in the matrix elements).[20,21] Weak transitions are usually subject to cancellation between various contributions and thus they are not normally capable of being reproduced with accuracy. We are usually satisfied if the calculated values are also weak. $E1$ transitions are always a problem, but especially so in the $A \sim 40$ region, where the active nucleons are mainly in the $d_{3/2}$ and $f_{7/2}$ orbits between which $E1$ transitions are forbidden. However, we do not wish to discount entirely our ability to calculate $E1$ (and $E1$-like) transitions. For example, the SDPF interaction has been used with considerable success in the prediction of nonunique first-forbidden matrix elements[19] which are dominated by $E1$-like matrix elements and thus depend on that part of our interaction which is not $d_{3/2}$-$f_{7/2}$. A point of interest will be how well we do with $E1$ transitions.

E. Binding energies

In the full SDPF model space the ^{39}Ar odd-parity ($1\hbar\omega$) spectrum extends to $J^\pi = \frac{15}{2}^-$ and has a maximum J dimension of 43 at $J^\pi = \frac{5}{2}^-$. The even-parity ($2\hbar\omega$) spectrum extends to $J^\pi = \frac{25}{2}^+$ and has a maximum J dimension of 3862 at $J^\pi = \frac{7}{2}^+$. With the computer resources available to us, we were just able to diagonalize the $J^\pi = \frac{7}{2}^+$ matrix. The odd- and even-parity spectra—which we shall label as $1\hbar\omega$ and $2\hbar\omega$—are listed in Table I. The $E_{B\,\text{corr}}$ of Table I are binding energies with the Coulomb contribution subtracted. For the shell-model prediction this is just the calculated binding energy since the SDPF interaction does not include the Coulomb interaction. The experimental value of $E_{B\,\text{corr}}$ is obtained for the ^{39}Ar $\frac{7}{2}^-$ ground state by adding to Wildenthal's[22] $E_{B\,\text{corr}}$ for ^{39}K the excitation energy of 6546(2) keV corresponding to the $J^\pi;T = \frac{7}{2}^-;\frac{3}{2}$ analog of the ^{39}Ar ground state in ^{39}K (Ref. 6). The $E_{B\,\text{corr}}$ for the $\frac{3}{2}{}_1^+$ level of ^{39}Ar is then obtained by adding its excitation energy of 1518 keV in ^{39}Ar (Ref. 6).

III. COMPARISON TO EXPERIMENT

A. The energy spectra

In Fig. 1 we compare the yrast states generated by the SDPF interaction with the known high-spin states of ^{39}Ar, while in Fig. 2 the low-lying spectra are considered. The spin-parity assignments given to the experimental levels follow Endt and van der Leun[6] with the exception of the yrast states at 2651, 3992, 4543, and 5535 keV. The assignments for these states are discussed in Appendix A.

Our first concern is a comparison of the absolute binding energies with experiment. As shown in Table I, the lowest $1\hbar\omega$ state (the $\frac{7}{2}{}_1^-$ level) is in almost perfect agreement: the prediction is 54 keV too bound. Granted the indicated correspondences between the experimental and predicted levels (to be discussed), the predicted and experimental $1\hbar\omega$ spectra are in very good agreement. For the even-parity states the binding energies of the high-spin levels are in excellent agreement, but the low-spin predictions are considerably overbound.

B. The yrast spectrum

The γ-ray cascade commencing with the depopulation of the 5535-keV level is the result of a fusion-evaporation study.[23,24] No other γ rays were observed in this study. The fusion-evaporation reaction is almost exclusively selective of yrast states. The calculations very nicely explain the main features of the spectrum; namely, the change in parity between the $\frac{11}{2}^-$ and $\frac{13}{2}^+$ states and the failure to observe higher spin states ($J > \frac{17}{2}$). The even-parity states become the yrast states at $J=\frac{13}{2}$ because of the very large energy gap between the $\frac{11}{2}^-$ and $\frac{13}{2}^-$ states (see Table I), due to the required participation of the $d_{5/2}$ orbit for $J^\pi > \frac{11}{2}^-$. The failure to observe higher spin states can be attributed to the fairly large gap between the $\frac{17}{2}^+$ and $\frac{19}{2}^+$ states. The cross section for forming the $\frac{19}{2}^+$ state will be down considerably as is the efficiency for detecting its γ decay (also see the discussion of Table II below).

We are interested in how well the SDPF can reproduce the observed γ-ray decay data. Accordingly, a comparison of experiment and theory is made in Table II. The notation used in Table II is used throughout this paper; namely, a number in parentheses following a predicted or experimental quantity has a + or − sign if it is a power of 10, and has no ± sign if it is the uncertainty in the least

TABLE I. The $(2s,1d)^{22}(fp)^1$ $1\hbar\omega$ spectra (left) and $(2s,1d)^{21}(fp)^2$ $2\hbar\omega$ spectra (right) of ^{39}Ar from the SDPF interaction. All $T=\frac{3}{2}$ levels are included up to the first No.$=10$; above that only yrast levels (No.$=1$) are listed. The predicted and experimental $E_{B\,\mathrm{corr}}$ are given in the first row.

E(theor) (MeV)	$2J^\pi$	No.	E(expt) (MeV)	E(theor) (MeV)	$2J^\pi$	No.	E(expt) (MeV)
−257.688	7^-	1	−257.634	−256.891	3^+	1	−256.116
1.330	3^-	1		1.016	1^+	1	
2.084	5^-	1		1.291	7^+	1	
2.133	9^-	1		1.548	3^+	2	
2.429	7^-	2		1.658	5^+	1	
2.443	3^-	2		2.087	1^+	2	
2.645	11^-	1		2.643	3^+	3	
3.056	1^-	1		2.718	11^+	1	
3.553	7^-	3		2.783	7^+	2	
3.583	5^-	2		2.865	5^+	2	
3.596	3^-	3		2.876	9^+	1	
4.223	9^-	2		3.060	3^+	4	
4.340	1^-	2		3.096	13^+	1	
4.527	7^-	4		3.134	7^+	3	
4.584	5^-	3		3.165	1^+	3	
4.780	11^-	2		3.182	11^+	2	
5.277	7^-	5		3.203	5^+	3	
5.405	3^-	4		3.460	3^+	5	
5.463	5^-	4		3.518	15^+	1	
5.672	5^-	5		3.556	3^+	6	
5.895	3^-	5		3.695	5^+	4	
6.058	7^-	6		3.732	1^+	4	
6.154	9^-	3		3.761	5^+	5	
6.345	5^-	6		3.775	7^+	4	
6.461	5^-	7		3.780	11^+	3	
6.696	3^-	6		3.819	9^+	2	
6.962	7^-	7		3.839	3^+	7	
7.043	1^-	3		3.864	7^+	5	
7.442	3^-	7		4.081	5^+	6	
7.459	1^-	4		4.187	13^+	2	
7.844	5^-	8		4.234	9^+	3	
7.993	9^-	4		4.260	7^+	6	
8.161	7^-	8		4.272	9^+	4	
8.167	11^-	3		4.280	7^+	7	
8.173	13^-	1		4.307	11^+	4	
8.254	5^-	9		4.364	9^+	5	
8.480	3^-	8		4.394	5^+	7	
8.523	9^-	5		4.439	3^+	8	
8.727	3^-	9		4.491	5^+	8	
8.857	7^-	9		4.533	3^+	9	
8.885	1^-	5		4.538	11^+	5	
9.103	3^-	10		4.562	7^+	8	
9.110	15^-	1		4.573	9^+	6	
				4.621	11^+	6	
				4.621	1^+	5	
				4.735	7^+	9	
				4.748	3^+	10	
				4.789	17^+	1	
				6.623	19^+	1	
				11.005	21^+	1	
				11.817	23^+	1	
				20.218	25^+	1	

significant figure. Asymmetric uncertainties are given as (upper/lower).

First consider the $\frac{7}{2}{}_1^+$ and $\frac{9}{2}{}_1^-$ levels. From Fig. 2 we see that for both of these levels there are two candidates amongst the known experimental levels below 3.4-MeV excitation. These candidates are the 2342- and 2524-keV levels, both of which were fixed as $\frac{5}{2}^-$, $\frac{7}{2}$, or $\frac{9}{2}^-$ by Sterrenburg *et al.*,[25] who reported the results shown for these two levels in Fig. 1 and Table II. These results are discussed in Appendix A. Almost all the known properties of these two levels are similar enough so that it is hard to choose which is $\frac{7}{2}^+$ and which $\frac{9}{2}^-$. We make the choice shown because the angular correlation results (Appendix A) give a poor fit ($\chi^2 > 3.5$) with $J^\pi = \frac{7}{2}^+$ for the 2524-keV level unless the $M2$ component in the 2524→0 transition has a strength $\gtrsim 1.5$ W.u. Such a large strength is unlikely in any event and especially in view of our prediction of 0.035 W.u. (see Table II). We note that if the correspondence were reversed so that the 2342-keV level was $\frac{9}{2}^-$ and the 2524-keV level was $\frac{7}{2}^+$, the quality of the agreement to the SDPF electromagnetic predictions would be improved for each level by about a factor of 2. With the present choice, we do not regard the disagreement in the $\frac{7}{2}^+ \rightarrow \frac{7}{2}^-$ $E1$ rate as serious. As was discussed in Sec. II D, we do not expect to calculate small $E1$ rates with any accuracy. The $M1$ strength of the $\frac{9}{2}^- \rightarrow \frac{7}{2}^-$ transition is predicted to be ~ 6 times too large, which is adequate for a quite small matrix element. The most serious discrepancy is in the $E2$ component of the $\frac{9}{2}{}_1^- \rightarrow \frac{7}{2}{}_1^-$ transition. We return to this subject below.

For the higher-spin yrast states the predicted branching ratios nicely reproduce the experimental situation; i.e., no $E2$ crossovers are observed. However, for the unobserved $\frac{19}{2}^+$ state the crossover is predicted to be dominant. Because of the inverse dependence of detection efficiency with γ-ray energy, this would render formation of the $\frac{19}{2}^+$ state even more difficult to observe. The strengths of the dipole decays predicted for the $\frac{13}{2}^+$, $\frac{15}{2}^+$, and $\frac{17}{2}^+$

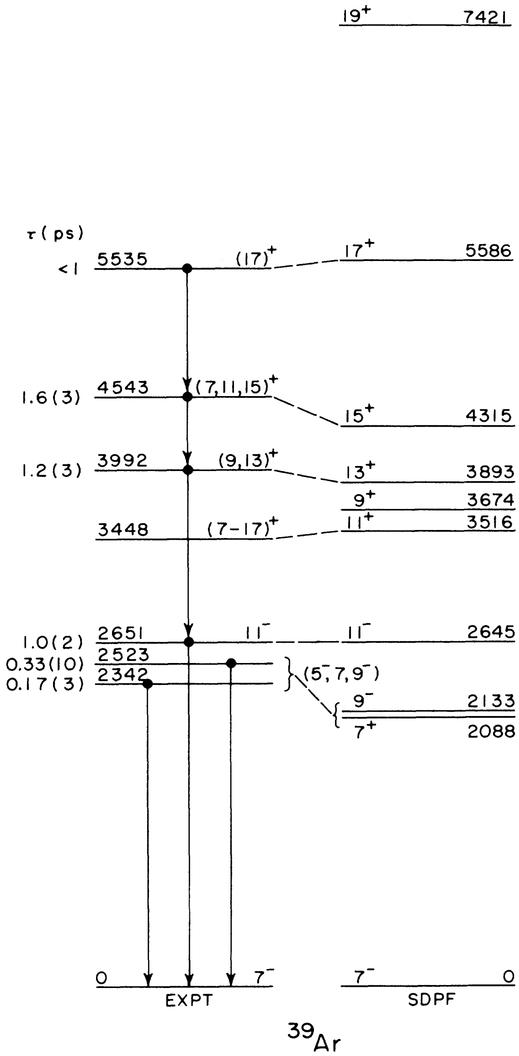

FIG. 1. Yrast spectra of ^{39}Ar. Levels are labeled by $2J^\pi$. The lowest-lying predicted levels with $2J \geq 7$ are shown for both even and odd parity up to 8-MeV excitation. The experimental data are either from Endt and van der Leun (Ref. 6) or are discussed in Appendix A.

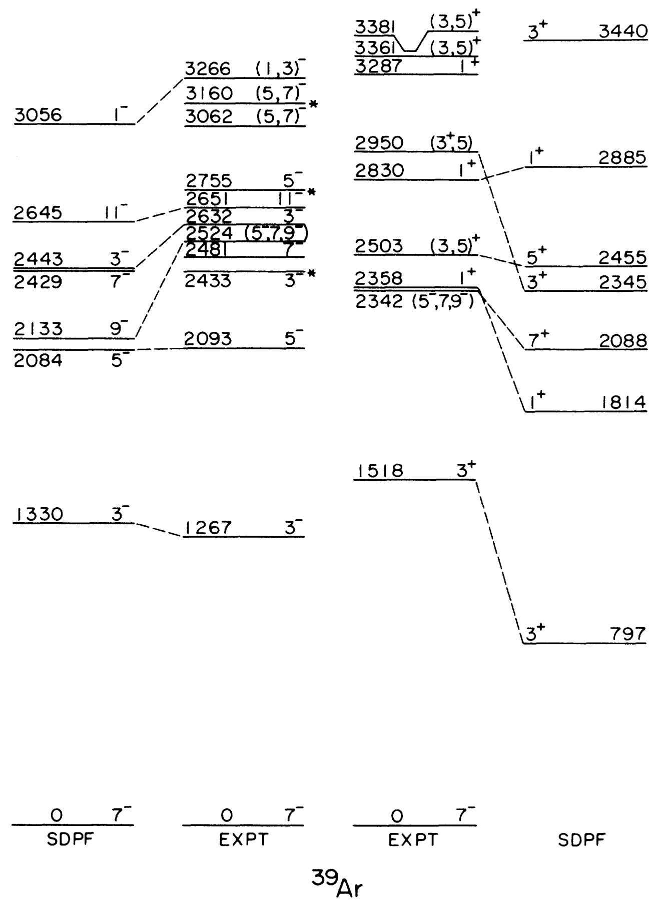

FIG. 2. The low-lying levels of ^{39}Ar. Levels are labeled by $2J^\pi$. All predicted and experimental levels up to 3.4-MeV excitation are included. The experimental data are from Endt and van der Leun (Ref. 6) or are discussed in Appendix A. The indicated correspondences between the calculated and experimental levels are discussed in the text. Levels proposed as intruders, i.e., predominantly from configurations outside our model space, are labeled by asterisks and are also discussed in the text.

states are in adequate agreement with experiment. It would be of interest to understand these decays in terms of the wave functions of these levels; however, this is difficult to do with an m-scheme shell-model program. The reader is referred to the quite illuminating discussion of these states given by Keinonen *et al.*;[24] our results tend to support their intuitive picture of these yrast states.

The $E2$ $\frac{11}{2}{}_1^- \rightarrow \frac{7}{2}{}_1^-$ transition is predicted to be 3.4 times stronger than is observed. This discrepancy is reminiscent of that for the $E2$ component of the $\frac{9}{2}{}_1^- \rightarrow \frac{7}{2}{}_1^-$ transition alluded to above. Keinonen *et al.*[24] discussed the $\frac{11}{2}{}_1^- \rightarrow \frac{7}{2}{}_1^-$ transition in terms of an extreme weak-coupling picture. In this model the $E2$ strength should be equal to that of the ^{38}Ar $2^+ \rightarrow 0^+$ core transition. The ^{38}Ar $E2$ strength is 3.0(2) W.u., which is in fair agreement with our prediction for the $\frac{11}{2}{}_1^- \rightarrow \frac{7}{2}{}_1^-$ transition; i.e., our results are in accord with the weak-coupling picture. $E2$ transitions of moderate and higher strength are among the most reliable predictions of shell-model calculations. Thus failure to reproduce these two $E2$ rates in ^{39}Ar is a clear signal of either experimental difficulties or strong departures from the assumed shell-model configurations (and from a weak-coupling description).

C. The low-lying spectra

1. Spectroscopic factors

The $1\hbar\omega$ levels. The SDPF predictions for the single-neutron spectroscopic factors of $^{38}\mathrm{Ar} + \mathrm{n} \rightarrow {}^{39}\mathrm{Ar}$, S_n^+, and $^{40}\mathrm{Ar} - \mathrm{n} \rightarrow {}^{39}\mathrm{Ar}$, S_n^-, are listed in Table III for the first five states of the relevant J^π. S_n^- values for the odd-parity states are not listed. They are all negligible ($S_n^- < 0.01$) except for $\frac{7}{2}{}_1^-$ and $\frac{3}{2}{}_1^-$. The values for these two states are included in the comparison to experiment of Table IV. The experimental values in Table IV are taken from the evaluation of Endt[26] when given. Otherwise they are our estimates of the best values and uncertainties of the data compiled by Endt and van der Leun.[6]

The SDPF predictions for the $1\hbar\omega$ states are very similar (relative to the experimental uncertainties) to the previous results of Woods[4] and Gloeckner *et al.*[3] This is not surprising since spectroscopic factors are not as sensitive to truncation of the model space and variation of the ef-

TABLE II. ^{39}Ar yrast decays, theory (SDPF) and experiment (Expt.).

Initial state		Final state				$M(\lambda)^b$	$B(\lambda)^b$		Branching ratio (%)	
$2J^{\pi a}$	E_x (keV)	$2J^{\pi a}$	E_x (keV)	E_γ (keV)	λ	SDPF	SDPF	Expt.[c]	SDPF	Expt.
7^+	2342	7^-	0	2342	$E1$	−1.490[−2]	3.744[−5]	3.9(7)[−4]	100	100
					$M2$	2.297[+0]	3.475[−2]			
							$x=-0.033$	$x=-0.10(17)$		
9^-	2524	7^-	0	2524	$M1$	−7.808[−1]	3.405[−2]	5.4(17)[−3]	100	100
					$E2$	2.026[+1]	5.224[+0]	2.8(17)[−1]		
							$x=-0.55$	$x=-0.32(10)$		
11^-	2651	7^-	0	2651	$E2$	1.600[+1]	2.715[+0]	0.79(16)	96.9	100
		9^-	2342		$M1$	1.874[+0]	1.634[−1]		3.1	
11^+	3448	9^-	2342		$E1$	5.169[−2]	3.003[−4]		97.3	
		11^-	2651		$E1$	1.406[−2]	2.222[−5]		2.7	
13^+	3992	11^-	2651	1341	$E1$	8.559[−2]	7.059[−4]	2.9(7)[−4]	100	100
15^+	4543	11^+	3448	1095	$E2$	1.710[+1]	2.326[+0]		0.3	
		13^+	3992	551	$M1$	−2.374[+0]	1.967[−1]	1.2(2)[−1]	99.7	100
					$E2$	1.852[+1]	2.728[+0]			
							$x=-0.01$	$\lvert x \rvert < 0.07$		
17^+	5535	13^+	3992	1543	$E2$	1.845[+0]	2.407[−2]		0.1	
		15^+	4543	992	$M1$	1.949[+0]	1.179[−1]	$>0.32[-1]$	99.9	100
					$E2$	7.556[+0]	4.037[−1]			
19^+	(7421)[d]	15^+	4543	2878	$E2$	2.391[+1]	3.638[+0]		82.1	
		17^+	5535	1886	$M1$	−4.733[−1]	6.256[−3]		17.9	
					$E2$	2.485[+0]	3.929[−2]			
							$x=-0.02$			

[a]Not necessarily established, but assumed for present considerations.

[b]The units of $M(\lambda)$ are $\mu_N \mathrm{fm}^{L-1}$ and $e\,\mathrm{fm}^L$ for ML and EL transitions, respectively. The units of $B(\lambda)$ are Weisskopf units (W.u.). $M(\lambda)^2=(2J_i+1)B(\lambda)$. For the SDPF predictions, the power of 10 is given in square brackets as denoted by giving the sign (+ or −) explicitly.

[c]Values in parentheses give the uncertainty in the least significant figure; those in square brackets are the power of 10, i.e., $-1.490[-2] = -1.490 \times 10^{-2}$. See Appendix A for a discussion of the data.

[d]The SDPF prediction.

TABLE III. Predicted $(2J+1)S_n^+$ spectroscopic factors for the reaction ^{38}Ar(d,p)^{39}Ar leading to $1\hbar\omega$ states and S_n^- spectroscopic factors for ^{40}Ar(p,d)^{39}Ar leading to $2\hbar\omega$ states. The first fives states, ordered by energy, are listed for each J.

	$(2J+1)S_n^+$ $2J^\pi$				S_n^- $2J^\pi$		
State	1^-	3^-	5^-	7^-	1^+	3^+	5^+
1	1.06	3.05	0.06	7.10	0.170	2.88	0.045
2	0.91	0.71	6.4[−4]	0.78	0.657	0.251	0.319
3	5.0[−4]	0.05	0.07	0.13	0.021	0.033	0.070
4	1.3[−3]	0.08	0.09	0.05	0.202	2.7[−3]	0.132
5	1.3[−3]	0.07	3.2[−3]	0.03	0.015	3.3[−3]	0.079

fective interaction as the matrix elements of dipole γ transitions and beta-decay can be. The agreement with experiment for the $1\hbar\omega$ states (Table IV) is quite satisfactory up to 3-MeV excitation if we identify the 2433-keV level as an intruder (presumably $3\hbar\omega$). Woods came to the same conclusion regarding this state. The evidence for this identification is not only from Table IV, but also from the energy spectra of Fig. 2. Here we see that there are too many experimental odd-parity levels in ^{39}Ar below 3-MeV excitation relative to the $1\hbar\omega$ calculation. If there is a low-lying $\frac{3}{2}^-$ $3\hbar\omega$ state then—from the known systematics of neighboring nuclei (see Table V)—we expect low-lying $\frac{5}{2}^-$ and $\frac{7}{2}^-$ states as well. Candidates for these two states are also indicated (asterisks) in Fig. 2.

It can be inferred from Table III (with the aid of Table I) that the only appreciable S_n^+ strength predicted to lie in the region of excitation between ~ 3 and 6 MeV belongs to the $\frac{1}{2}{}_1^-$ and $\frac{1}{2}{}_2^-$ states. Experimentally, two states with appreciable $l_n=1$ spectroscopic strength have been observed in this region in three different investigations.[27–29] The weighted average excitation energies of the states involved from two of these studies[27,29] are 3258(9) and 4375(9) keV. There is no evidence ruling against a $\frac{1}{2}^-$ assignment for the 4375-keV level. The 3258-keV level is another matter. Sterrenburg *et al.*[25] measured angular correlations in the ^{38}Ar(d,pγ)^{39}Ar reaction and found an anisotropic angular distribution for a $3266\rightarrow 0$ γ transition, thus ruling out $J=\frac{1}{2}$ for the state they placed at 3265.6(3) keV. On the other hand, Fitz *et al.*[28] and Sen *et al.*[29] assigned $\frac{1}{2}^-$ to the 3258-keV level on the basis of the observed (d,p) angular distribution and the Lee-Schiffer effect.[30] Our predictions strongly support the $\frac{1}{2}^-$ assignment of Fitz *et al.*[28] and of Sen *et al.*[29] The solution to the discrepancy may be the existence of a $\frac{1}{2}^-,\frac{3}{2}$ doublet at 3.27 MeV in ^{39}Ar. The $\frac{1}{2}^-$ state would then be responsible for the observed $l_n=1$ (d,p) angular distribution, while at backangles ($\theta_p=160°-172°$), where the protons were detected in the (d,pγ) experiment, both members of the doublet could be involved. It is also possible, but less likely, that the (d,pγ) experiment[25] is in error. We anticipate the discussion of electromagnetic decays to note that the SDPF prediction for the γ decay of the $\frac{1}{2}{}_1^-$ state—if it is at 3258 keV—is for a mean life of 9 fs and branching ratios ($>0.1\%$) of 98.8% and 1.1% to $\frac{3}{2}{}_1^-$ and $\frac{3}{2}{}_2^-$. These predictions happen to be in excellent accord with the known decay modes of the 3266-keV level as observed by Sterrenburg *et al.*[25]

The $2\hbar\omega$ levels. The nonzero experimental S_n^+ values

TABLE IV. Experimental single-neutron stripping (S_n^+) and pickup (S_n^-) spectroscopic factors for ^{39}Ar levels.

Experimental[a]					SDPF[b]			
$2J^\pi$	E_x (keV)	l_n	$(2J+1)S_n^+$	S_n^-	$2J_k^\pi$	E_x (keV)	$(2J+1)S_n^+$	S_n^-
7^-	0	3	5.1(10)	1.2(2)	7_1^-	0	7.10	1.85
3^-	1267	1	2.28(36)	0.10(2)	3_1^-	1330	3.05	0.09
3^+	1518	2	0.24(12)	2.0(3)	3_1^+	797		2.88
5^-	2093	3	0.10(3)	0.08(5)	5_1^-	2084	0.06	0.00
1^+	2358	0	0.06(2)	1.0(4)	1_1^+	1813		0.17
3^-	2433	1	0.09(4)		c	c	c	c
7^-	2482	3	0.62(15)		7_2^-	2429	0.78	0.00
$(3,5)^+$	2503	2			5_1^+	2455		0.05
3^-	2631	1	0.82(15)	0.03(2)	3_2^-	2443	0.71	0.00
1^+	2830	0		0.02(2)	1_2^+	2884		0.66
3^-	3266	1	1.0(20)		1_1^-	3056	1.06	0.00
1^+	3287	0		0.19(10)	1_3^+	3962		0.02
$(1,3)^-$	4375	1	0.80(20)		1_2^-	4340	0.91	0.00

[a]From Ref. 21 when given; otherwise our estimate of the best value from the data compiled in Ref. 6.
[b] J_k^π is chosen to best describe the data; the choice is discussed in the text. k orders the levels of J^π by energy.
[c]Assumed to be a $3\hbar\omega$ intruder.

TABLE V. Probable low-lying intruder states in some $A=39$–45 nuclei.

Nucleus	$J^\pi = \frac{3}{2}^-$	E_x (keV) $\frac{5}{2}^-$	$\frac{7}{2}^-$
^{39}Ar	2433	2756	3160
^{41}Ca	2330[a]	2575	2959
^{43}Ca	2103	1931	2067
^{43}Sc	472	845	1408
^{45}Sc	377	720	1409

[a]Mixture of the 1943- and 2462-keV levels which share the S_n^+ $p_{3/2}$ spectroscopic strength.

for the $\frac{3}{2}{}_1^+$ and $\frac{1}{2}{}_1^+$ levels signal $2\hbar\omega$ admixtures in the ^{38}Ar ground state and remind us of the deficiencies of our model space and the expected presence of $3\hbar\omega$ admixtures in the $1\hbar\omega$ levels.

The S_n^- predictions for the known or possible $\frac{3}{2}^+$ and $\frac{5}{2}^+$ states agree satisfactorily with experiment. We note the same trend as for the $1\hbar\omega$ states; i.e., the calculations give values somewhat too large for both S_n^+ and S_n^-. This suggests a sharing of the spectroscopic strength with intruder states. For the $\frac{1}{2}^+$ states we have a serious disagreement with experiment for the distribution of strength. However, the summed S_n^- strength to the lowest three $\frac{1}{2}^+$ states is 1.2(4) experimentally and 0.85 calculated, in satisfactory agreement. It would appear that the SDPF interaction somehow admixes these three states incorrectly.

2. *Electromagnetic decays*

Comparison between theory and experiment for the electromagnetic transitions connecting the low-lying states of ^{39}Ar is complicated by indefinite spin-parity assignments and by the probable presence of intruder states. Because of these factors we give, for present and future use, rather extensive lists of electromagnetic matrix elements. These are collected in Appendix B. Comparison is also difficult for those levels with unknown mean lives. (A compilation of lifetime information for the low-lying states of ^{39}Ar is included in Appendix A.) Ideally, we prefer a comparison to transition strengths (or even better, matrix elements) of definite multipolarities and we make this comparison when possible. For levels with unknown lifetimes we are reduced to a comparison of branching ratios. We start our comparison with the ground state and first two odd-parity excited states.

The ground state, 1267-, and 2093-keV levels. The magnetic moment of the $\frac{7}{2}^-$ ground state is -1.80 μ_N according to the SDPF and $-1.3(3)$ μ_N, experimentally (Ref. 6).

The 1267-keV $\frac{3}{2}^-$ first-excited state is predicted to decay by an $E2$ transition of 3.20 W.u. corresponding to a meanlife of 9.9 ps as compared to the experimental limit of <700 ps.

For the third-excited $\frac{5}{2}^-$ 2093-keV level we find a meanlife of 30 fs compared to the experimental limit <50 fs. The branching ratios are calculated to be 95.2%, 4.6%, and 0.2% to $\frac{7}{2}{}_1^-$, $\frac{3}{2}{}_1^-$, and $\frac{3}{2}{}_1^+$, respectively. Experimentally, these are 96.1(8)%, 3.9(8)%, and <0.7%. The $\frac{5}{2}^- \to \frac{7}{2}^-$ $E2/M1$ mixing ratio is $+0.17$ from the SDPF and $+0.21(6)$ experimentally. It can be said that the agreement for these three levels is excellent.

The 2632- and 2481-keV levels. Of the states associated with the $1\hbar\omega$ model space in Fig. 2, these are the only ones below 3-MeV excitation whose γ decay we have not yet discussed. Results pertaining to the γ decay of these two levels are collected in Table VI. For the 2632-keV level the agreement with an assignment as $\frac{3}{2}{}_2^-$ is satisfactory. Weak transitions are predicted as such and the only relatively large $B(\lambda)$—that for the $M1$ 2632$\to$2093 transition—is reproduced within a factor of ~ 2.

For the 2481-keV level the agreement is quite good. The distinctive factor in the decay of this level is the almost vanishing $M1$ component in the ground-state branch. We see that the prediction is also for a very small $M1$ strength, and the moderate $E2$ strength is reproduced. The moderately strong 2481$\to$2093 $M1$ strength is also reproduced to within a factor of 2. Note that so far there are no disagreements in the signs of $x(L+1/L)$ mixing ratios.

The 1518-, 2503-, and 2950-keV levels. Electromagnetic decay results for these three levels are collected in Table VII. For the $\frac{3}{2}{}_1^+$ 1518-keV level the strong $M2$ ground-state decay is reproduced quite well, but $x(E2/M2)$ is about 4 times too small, indicating poor agreement for the $E3$ matrix element.

The 2503- and 2950-keV levels are the only two candidates below 3.3-MeV excitation for the $\frac{3}{2}{}_2^+$ and $\frac{5}{2}{}_1^+$ states predicted at 2345 and 2455 keV, respectively. The identification of the 2503-keV level as $\frac{5}{2}{}_1^+$ and the 2950-keV level as $\frac{3}{2}{}_2^+$ is tested in Table VII. The most dominant matrix element in the decay of these two levels is that for the $M1$ $\frac{3}{2}{}_1^+ \to \frac{5}{2}{}_1^+$ transition. This is reproduced very well by the calculation, but we note that the same dominance would pertain if the identification were reversed. A strong disagreement exists for the 2503$\to$0 transition, but the overall agreement is quite satisfactory. Note that once again the signs of the predicted mixing ratios are consistent with observation.

If we reversed the identification of the levels so that the 2950- and 2503-keV levels were $\frac{5}{2}^+$ and $\frac{3}{2}^+$, respectively, the agreement is somewhat weakened, but not enough to make a good distinction between the two choices.

The 2358- and 2830-keV levels. These are the last two states below 3-MeV excitation whose γ decays we wish to consider. Both levels are assigned $\frac{1}{2}^+$ and we associate them with $\frac{1}{2}{}_1^+$ and $\frac{1}{2}{}_2^+$. Only lifetime limits are known. We calculate $\tau=5.6$ and 0.68 ps while the experimental limits are >0.6 and >1.0 ps, respectively. The only significant branches (>0.3%) for the 2358-keV level are calculated as 40% to the $\frac{3}{2}^-$ 1267-keV level and 60% to the $\frac{3}{2}^+$ 1518-keV level. Both the $E1$ and $M1$ rates are weak and thus unreliable. The $E1$ rate could easily be ~ 10 times larger, which would then give approximate agreement with the experimental branches of 94.9(4)% and 5.1(4)%, respectively. Significant branches (>0.3%)

from the 2830-keV level are calculated to be 35% to $\frac{3}{2}{}_1^-$ and 57% to $\frac{3}{2}{}_1^+$, as opposed to 49.2(8)% and 42.8(8)%, respectively. The agreement is good, but note the total radiative width thus predicted is 50% larger than the experimental limit.

We pointed out earlier that the predicted spectroscopic factors S_n^- for the $\frac{1}{2}^+$ states were strongly at odds with experiment. For instance, better agreement would result if the wave functions of the first two $\frac{1}{2}^+$ states were interchanged. In view of this, it is interesting to see if the electromagnetic decays can actually distinguish one state from another. If we reverse the wave functions associated with the 2358- and 2830-keV levels, then the 2358-keV level has a calculated meanlife of 2.4 ps and branches to the $\frac{3}{2}{}_1^-$ and $\frac{3}{2}{}_1^+$ states of 46% and 54%, respectively, while the 2830-keV level would have a calculated meanlife of 1.2 ps and branches to the $\frac{3}{2}{}_1^-$ and $\frac{3}{2}{}_1^+$ states of 25% and 75%, respectively. The agreement with experiment is just as good as observed previously. We conclude that the electromagnetic decay modes are relatively insensitive to interchange of the $\frac{1}{2}{}_1^+$ and $\frac{1}{2}{}_2^+$ wave functions and they do not give much help in understanding the structure of the 2358- and 2830-keV levels

3. $^{39}Cl(\beta^-)^{39}Ar$

Allowed decay. The predictions for the transition strengths of allowed GT decay of $J^\pi=\frac{3}{2}^+$ ^{39}Cl to the first five ^{39}Ar states of $\frac{1}{2}^+$, $\frac{3}{2}^+$, and $\frac{5}{2}^+$ are collected in Table VIII. Comparison to the experimental results of Ref. 7 (preceding paper) is made in Table IX. The most noticeable feature of these results is the smallness of B_0 values. The mean value for 10^3B_0 in the $(2s,1d)$ shell compilation of Ref. 18 is $\sim$600. For the small ^{39}Cl B_0 values good agreement with experiment in individual cases would be largely fortuitous; however, the summed GT strength, $\sum_f B_0$, for the first five states of Table IX is predicted to be $\sim$3 times too large and this may be a cause for concern.

An understanding of the weakness of these decays can be obtained by comparison to the sum-rule limit and to a hypothetical ^{37}Cl$(\beta^-)^{37}$Ar decay. For both ^{39}Cl and ^{37}Cl, the effect of Pauli blocking on β^+ decay is absolute for the $(2s,1d,1f,2p)$ model space, i.e., the summed β^+ transition strength is zero and the usual Gamow-Teller sum rule[18] becomes

$$\sum_f B_0=(1.26)^2\,3(N_i-Z_i)\ . \tag{4}$$

Summing over the fifteen final states of Table VIII, we find 1.4% of the sum rule. This a very small value indeed (compare Fig. 3 of Ref. 18). For the hypothetical ^{37}Cl$(\beta^-)^{37}$Ar decay to the first five $\frac{1}{2}^+$, $\frac{3}{2}^+$, and $\frac{5}{2}^+$ final states we find 13.4%—some 10 times more, but still quite small. We explain this reduction from ^{37}Cl to ^{39}Cl as follows: The ^{39}Cl decay is strongly dominated by $(2s,1d)$ transitions, with $(1f,2p)^2$ transitions hardly involved at all. [One reason for this is that the low-lying

TABLE VI. Electromagnetic decay of the 2632- and 2481-keV levels of ^{39}Ar. (BR denotes branching ratio.)

Initial state[a]		Final state[a]				$B(\lambda)$[b] or $x(L+1/L)$[c]		BR (%)	
$2J_k^\pi$	E_x (keV)	$2J_k^\pi$	E_x (keV)	E_γ (keV)	Quantity	Expt.	SDPF	Expt.	SDPF
3_2^-	2632	7_1^-	0	2632	$B(E2)$	<9.6[−3]	2.60[−1]	<0.7	15.6
		3_1^-	1267	1365	$B(M1)$	<7.7(4)[−4]	3.76[−6]	5.7(8)	0.4
					$B(E2)$	<1.3(8)[+1]	1.45[−1]		
					$x(E2/M1)$		−4.68		
		3_1^+	1518	1114	$B(E1)$	8(5)[−5]	4.11[−5]	13.4(10)	3.3
		5_1^-	2093	539	$B(M1)$	1.6(10)[−1]	3.31[−1]	81.0(20)	80.7
					$B(E2)$		5.93[−1]		
					$x(E2/M1)$	−0.07(14)	−0.01		
		τ(expt)=1.0(14/4) ps			τ(SDPF)=0.49 ps				
7_2^-	2481	7_1^-	0	2481	$B(M1)$	<3.0[−4]	3.46[−3]	82.5(6)	85.1
					$B(E2)$	1.8(7)[+0]	2.02[+0]		
					$x(E2/M1)$	+[0.14(10)]$^{-1}$	+1.10		
		3_1^-	1267	1214	$B(E2)$	<3.8	1.39	<3	0.9
		5_1^-	2093	389	$B(M1)$	1.9(7)[−1]	3.09[−1]	17.5(6)	14.0
					$B(E2)$	<1.0[+2]	1.75[+0]		
					$x(E2/M1)$	−0.03(12)	−0.02		
		τ(expt)=500(190) fs			τ(SDPF)=244 fs				

[a]The index k orders the states of a given J^π by energy. The E_x are the experimental states with which the shell-model states are identified for purposes of this comparison.
[b]The $B(\lambda)$ are in Weisskopf units.
[c]The phase convention is that of Rose and Brink (Ref. 15).

TABLE VII. Electromagnetic decays of the 1518-, 2503-, and 2950-keV levels of ^{39}Ar.

Initial state[a] $2J_k^\pi$	E_x (keV)	Final state[a] $2J_k^\pi$	E_x (keV)	E_γ (keV)	Quantity	$B(\lambda)$[b] or $x(L+1/L)$[c] Expt.	SDPF	BR (%) Expt.	SDPF
3_1^+	1518	7_1^-	0	1518	$B(M2)$	1.56(9)[−1]	1.70[−1]	45.9(8)	71
					$x(E3/M2)$	−20(4)	−0.05		
		3_1^-	1267	250	$B(E1)$	2.14(12)[−5]	0.79[−5]	54.1(8)	29
		τ(expt)=1.37(7) ns				τ(SDPF)=2.01 ns			
$5_1^{+\,d}$	2503	7_1^-	0	2503	$B(E1)$	≤9(3)[−8]	1.01[−4]	0.24(3)	0[e]
					$B(M2)$	≤7(2)[−2]	2.13[−1]		
		3_1^-	1267	1236	$B(E1)$	8.4(27)[−6]	9.12[−5]	2.7(2)	23
		3_1^+	1518	986	$B(M1)$	2.0(6)[−2]	1.83[−2]	12.8(2)	66
					$B(E2)$	4.8(22)[+0]	2.98[+0]		
					$x(E2/M1)$	−0.27(5)	−0.22		
		5_1^-	2093	411	$B(E1)$	3.6(12)[−4]	1.15[−3]	4.3(3)	11
		τ(expt)=1.45(45) ps				τ(SDPF)=1.14 ps			
$3_1^{+\,d}$	2950	7_1^-	0	2950	$B(M2)$	<1.3[+0]	4.44[−1]	<2	0.9
					$B(E3)$	<7.66[+2]	4.84[−1]		
		3_1^-	1267	1683	$B(E1)$	<3.4[−5]	1.40[−8]	<5	0.0
		3_1^+	1518	1433	$B(M1)$	1.13(64)[−2]	2.25[−2]	48.6(10)	72.4
					$B(E2)$	1.5(14)[+0]	1.20[+0]		
					$x(E2/M1)$	+0.29(18)	+0.18		
		5_1^-	2093	858	$B(E1)$	<2.1[−4]	6.6[−4]	<4	15.4
		$5_1^{+\,d}$	2503	447	$B(M1)$	4.3(25)[−1]	1.30[−1]	51.4(10)	12.3
					$B(E2)$		1.13[+0]		
					$x(E2/M1)$	>−0.27	+0.02		
		τ(expt)=430(400/170) fs				τ(SDPF)=336 fs			

[a]The index k orders the states of a given J^π by energy. The E_x are the experimental states to which the shell-model states are identified for purposes of this comparison.
[b]The $B(\lambda)$ are in Weisskopf units.
[c]The phase convention is that of Rose and Brink (Ref. 15).
[d]Assumed in this comparison.
[e]Assumed value.

TABLE VIII. ^{39}Cl$(\beta^-)^{39}$Ar Gamow-Teller transition strengths for the lowest five ^{39}Ar states of the three allowed J^π values. The two different results are described in the text. The index k orders the states of a given J^π by energy.

J^π	k	10^3B_0 (free)	10^3B_0 (effective)
$\frac{1}{2}^+$	1	67.4	37.3
	2	0.9	0.3
	3	45.1	27.3
	4	12.2	6.3
	5	0.2	0.2
$\frac{3}{2}^+$	1	86.3	49.2
	2	1.1	0.6
	3	1.3	0.6
	4	13.4	6.0
	5	146.4	86.1
$\frac{5}{2}^+$	1	35.2	20.6
	2	10.3	5.1
	3	19.1	11.0
	4	2.7	1.4
	5	120.0	73.2

TABLE IX. Comparison of the predicted Gamow-Teller strengths for ^{39}Cl$(\beta^-)^{39}$Ar with experimental results (Ref. 7). The identification of the experimental states is that of Fig. 2. The SDPF results are for an effective operator and are from Table VIII.

J_n^π	E_x (keV)	10^3B_0 Expt.	SDPF
$\frac{3}{2}^+_1$	1518	13.74(6)	49.2
$\frac{1}{2}^+_1$	2358	4.34(32)	37.3
$\frac{5}{2}^+_1$	2503	6.68(54)	20.6
$\frac{1}{2}^+_2$	2830	8.85(97)	0.3
$\frac{3}{2}^+_2$	2950	0.88(15)	0.6
$\frac{1}{2}^+_3$	3287	<10	27.3

TABLE X. First-forbidden nonunique beta decay of $\frac{3}{2}^+$ ^{39}Cl to ^{39}Ar $\frac{3}{2}^-$ and $\frac{5}{2}^-$ levels.

$2J^\pi$	E_x (keV)	f(expt)	f(SDPF)[a] HO	WS	Rank[b]	Remarks[b]
3^-	1267	8.3(30)[−2]	4.10[−2]	3.02[−2]	0,1,2	$R1+R2<0.03\cdot R0$
3^-	2433	<1.1[−4]	4.30[−5]	3.17[−5]	0.1,2	Assumed 3_2^-
3^-	2632	<5.3[−4]	4.24[−5]	3.08[−5]	0,1,2	Assumed 3_2^-
			8.30[−4]	5.75[−4]	0,1,2	Assumed 3_3^-
5^-	2093	<1.6[−4]	1.51[−4]	1.58[−4]	1,2	$R1<0.05\cdot R2$
5	2756	<9.6[−5]	8.12[−6]	9.53[−6]	1,2	Assumed 5_2^-

[a]HO and WS correspond to harmonic oscillator and Woods-Saxon radial wave functions, respectively.
[b]The tensor ranks of the matrix elements which can contribute to the transition. The matrix elements of rank 0, 1, and 2 are designated as $R0$, $R1$, and $R2$, respectively (see Ref. 17).

states of $(2s,1d)^{21}(1f,2p)^2$ are found to be dominated by wave functions with two neutrons in the $(1f,2p)$ shell.] Then the question reduces to the effect of the coupling of the two $(1f,2p)$ nucleons to the $A=37$ core. The J dimension for ^{37}Ar in the $(2s,1d)^{21}$ space is of order 20, as compared to order ~ 2000 in ^{39}Ar in the $(2s,1d)^{21}(1f,2p)^2$ model space. Clearly, the GT strength is spread over many more ^{39}Ar states and since the density of low-lying states is roughly the same for ^{37}Ar and ^{39}Ar, the expected strength energetically available to β^- decay is greatly reduced.

First-forbidden decay. The unique first-forbidden decay of $\frac{3}{2}^+$ ^{39}Cl to the $\frac{7}{2}^-$ ^{39}Ar ground state was satisfactorily explained by Towner *et al.*,[31] who started with a basic $(d_{3/2}f_{7/2})^7$ model space, but used perturbation theory to include the full $(2s,1d,1f,2p)$ space in the initial state and ground-state correlations in the final state. They obtained $B_1=1.1$ fm^2, as opposed to the experimental value of 1.3(4) fm^2. In our calculation, ground-state correlations in the final state are not included. From the work of Towner *et al.*[31] we know that ground-state correlations give a largely state-independent reduction of B_1 by a factor of

TABLE XI. Results extracted from the ^{36}S(α,nγ)^{39}Ar angular correlation measurements of Ref. 25.

E_i	J_i^π	E_f	J_f^π	$x(L+1/L)$	$\chi^2_{\min}$
2342	$\frac{5}{2}^-$	0	$\frac{7}{2}^-$	+1.0(5)	1.8
	$\frac{7}{2}$			−0.10(17)	0.0
	$\frac{9}{2}^-$			−0.47(6)	1.0
2503	$\frac{3}{2}^+$	1518	$\frac{3}{2}^+$	+0.13(10), or $\lvert x\rvert>4.7$	0.3, 0.2
	$\frac{5}{2}^+$			−0.27(5)	0.3
2524	$\frac{5}{2}^-$	0	$\frac{7}{2}^-$	−0.27(5)	2.5
	$\frac{7}{2}$			+0.23(7), or −1.7(4)	1.8, 1.3
	$\frac{9}{2}^-$			−0.32(10)	3.3
2651	$\frac{3}{2}^-$	0	$\frac{7}{2}^-$	$+0.09<x<1.2$	1.5
	$\frac{5}{2}^-$			$+0.27<x<2.0$	1.7
	$\frac{7}{2}^-$			$-2.3<x<+0.27$	0.0
	$\frac{9}{2}^-$			−0.36(14)	2.3
	$\frac{11}{2}^-$			+0.00(9)	0.07
2950	$\frac{3}{2}^+$	1518	$\frac{3}{2}^+$	+0.29(18), or $\lvert x\rvert>2.7$	0.0
	$\frac{5}{2}^+$			−0.06(6)	0.0
	$\frac{3}{2}^+$	2503	$\frac{5}{2}^+$	>-0.27	0.0
	$\frac{5}{2}^+$		$\frac{3}{2}^+$	−0.36(18)	0.07

$\sim$4.2 in $A\sim$37–43 nuclei. Applying this quenching to our calculation, we obtain $B_1=1.1$ fm^2 when harmonic oscillator radial wave functions are used and $B_1=1.2$ fm^2 for Woods-Saxon radial wave functions. These results are in nice agreement with Towner *et al.*[31] and with experiment.[7] The transition strength for the decay to $\frac{7}{2}{}_2^-$ (identified as the 2481-keV level) is calculated as $B_1\sim 0.13$ fm^2, which is consistent with the experimental limit of <0.8 fm^2 (Ref. 7). Predicted B_1 values to $\frac{7}{2}{}_k^-$ ($k=3,4,5$) states are 4.12×10^{-3}, 2.67×10^{-3}, and 7.31×10^{-3} fm^2, respectively.

Comparison with experiment for the nonunique first-forbidden decays to the possible $\frac{1}{2}^-$, $\frac{3}{2}^-$, $\frac{5}{2}^-$ states below 3.0-MeV excitation is made in Table X. The only observed branch, to the 1267-keV level, is explained quite well by the calculations. Note that the decay is dominated by a $2p_{3/2}\rightarrow 1d_{3/2}$ transition and so is a good test of that part of our interaction not involving the usually dominant $1f_{7/2}$ subshell. The other predictions are seen to be consistent with the experimental limits, especially if the 2433-keV level is identified as an intruder and the 2632-keV level as $\frac{3}{2}{}_2^-$, as we have done.

IV. SUMMARY

Our understanding of the nuclear structure of ^{39}Ar via the shell model has been extended by a calculation in the full $(2s,1d)(1f,2p)$ space for both odd- and even-parity states. The calculation explains the observed yrast spectra quite well. Comparison to experiment for the low-lying $1\hbar\omega$ states is complicated by the presence of "intruder" states which presumably arise from ^{16}O$(2s,1d)^{20}(1f,2p)^3$ configurations. Three of these states are identified with reasonable certainty. In our comparison to experiment we must keep in mind the possible effects of mixing between the $1\hbar\omega$ and $3\hbar\omega$ states, although, to some degree, our effective interaction includes some recognition of this mixing.

It is hoped that this study will stimulate further experimental work on the spectroscopy of ^{39}Ar. There is a general need for definite spin-parity assignments and level lifetime measurements. In addition, we have pinpointed one severe experimental discrepancy, namely the spin and (d,p) spectroscopic strength of the 3266-keV level. This discrepancy in the spectroscopic strength was noticed previously in a comparison of the even-parity states of ^{37}S-^{39}Ar-^{41}Ca (Ref. 34).

The agreement of our predicted electromagnetic rates with experiment is only fair. There are several unexplained discrepancies for $E2$ rates. $E1$ rates are extremely small experimentally and, not surprisingly, are predicted to be small. Other than this, the $E1$ predictions are essentially of no quantitative value. They are presumably influenced by admixtures of configurations from outside our configuration space and perhaps by spuriosity.

It appears to us that the next critical steps in our understanding of the spectroscopy of the low-lying states of ^{39}Ar are (1) the determination of spins, parities, and lifetimes, and (2) a reliable identification of intruder states, perhaps with the aid of multinucleon transfer reactions such as ^{36}Ar(^{18}O,^{15}O)^{39}Ar and ^{36}S$(\alpha,$n$)^{39}$Ar as well as via model calculations.

TABLE XII. ^{39}Ar spin-parity and mean lifetimes from Appendix A or Ref. 6.

E_x (keV)	J^π	τ
1267	$\frac{3}{2}^-$	<0.7 ns
1518	$\frac{3}{2}^+$	1.37(7) ns
2093	$\frac{5}{2}^-$	<50 fs
2342	$\frac{5}{2}^-,\frac{7}{2},\frac{9}{2}^-$	170(30) fs
2358	$\frac{1}{2}^+$	>600 fs
2433	$\frac{3}{2}^-$	1.00(45/20) ps
2481	$\frac{7}{2}^-$	500(190) fs
2503	$\frac{3}{2}^+,\frac{5}{2}^+$	1.45(45) ps
2524	$\frac{5}{2}^-,\frac{7}{2},\frac{9}{2}^-$	330(100) fs
2632	$\frac{3}{2}^-$	1.0(14/4) ps
2651	$\frac{11}{2}^-$	1.0(2) ps
2756	$\frac{5}{2}^-$	170(60) fs
2830	$\frac{1}{2}^+$	>1.0 ps
2950	$\frac{3}{2}^+,\frac{5}{2}$	430(400/170) fs
3062	$\frac{5}{2}^-,\frac{7}{2}^-$	150(40) fs
3160	$\frac{5}{2}^-,\frac{7}{2}^-$	2.0(20/7) ps
3266	$\frac{1}{2}^-,\frac{3}{2}^-$	<70 fs
3287	$\frac{1}{2}^+$	360(400/150) fs

ACKNOWLEDGMENTS

I thank J. A. Becker for assistance with the computing and for many helpful discussions. Both J. A. Becker and J. W. Olness are to be thanked for a critical reading of the manuscript. This research was supported by the U.S. Department of Energy under Contract No. DE-AC02-76CH00016.

APPENDIX A: ANALYSIS OF SOME PREVIOUS EXPERIMENTS

1. ^{36}S$(\alpha,$n$\gamma)^{39}$Ar angular correlation measurements

A very important contribution to the spectroscopy of the low-lying ^{39}Ar levels is the ^{36}S$(\alpha,$n$\gamma)^{39}$Ar angular correlation and level lifetime study of Sterrenburg *et al.*[25] The $(\alpha,$n$\gamma)$ correlations were measured in a collinear geometry and were analyzed to give unambiguous spin-parity assignments to eight ^{39}Ar states below 3.3-MeV excitation. Multipole mixing ratios, $x(L+1/L)$, were also given for the main γ-ray decays of these levels. For seven other levels ambiguities remain in the spin-parity assignments and $L+1,L$ mixing ratios were not explicitly given. However, the angular distribution coefficients from a Legendre polynomial expansion were given and thus it is possible to extract mixing ratios for various assumptions of the spins involved.[32] These mixing ratios provide information which we wish to compare to the

TABLE XIII. Electromagnetic matrix elements, $M(\lambda)$, between $1\hbar\omega$ of ^{39}Ar. The units and definition of $M(\lambda)$ are given in the text. When allowed, $M1$ (top) and $E2$ (bottom) matrix elements are given; otherwise the allowed $M(\lambda)$ is given.

			$M(\lambda)$				
					n_f		
J_f^π	J_i^π	n_i	1	2	3	4	5
$\frac{1}{2}^-$	$\frac{1}{2}^-$	1		1.981[−1]	2.806[−1]	3.966[−2]	8.593[−3]
		2			2.792[−1]	8.877[−2]	5.316[−2]
		3				1.089[+0]	4.891[−2]
$\frac{3}{2}^-$	$\frac{1}{2}^-$	1	+1.248[+0]	+7.505[−1]	−1.083[+0]	+1.346[−1]	+6.952[−1]
			9.145[+0]	1.371[+0]	1.656[+0]	2.066[+0]	5.856[+0]
		2	−8.365[−1]	+1.279[−1]	−1.387[+0]	+9.371[−2]	−1.064[+0]
			2.657[+0]	2.541[+0]	1.226[−2]	2.730[+0]	6.790[+0]
		3	−3.305[−2]	+1.544[−1]	−3.012[−1]	−2.137[−2]	+1.160[−1]
			3.137[+0]	1.326[+0]	8.000[+0]	4.688[+0]	6.147[−1]
$\frac{3}{2}^-$	$\frac{3}{2}^-$	1		−5.188[−3]	+1.484[−1]	+1.720[−1]	+4.436[−2]
				2.132[+0]	9.243[+0]	2.734[−1]	4.583[−1]
		2			+3.112[−1]	−2.968[−1]	+1.471[−1]
					1.592[−1]	6.369[−1]	2.817[−1]
		3				−9.855[−1]	−1.138[+0]
						2.208[+0]	6.475[−1]
$\frac{3}{2}^-$	$\frac{5}{2}^-$	1	+9.693[−1]	−1.540[+0]	−3.608[−1]	+1.348[+0]	+5.059[−1]
			1.471[+0]	4.317[+0]	4.044[+0]	6.129[+0]	1.245[+0]
		2	−2.895[−2]	+2.596[−2]	−2.095[+0]	−3.728[−1]	−1.063[+0]
			1.070[+1]	2.269[+0]	3.254[+0]	5.207[−1]	4.378[+0]
		3	−3.708[−1]	−3.680[−1]	−4.293[−1]	+2.552[+0]	+1.429[−1]
			2.774[+0]	6.989[+0]	1.788[+0]	2.524[−1]	2.892[+0]
$\frac{3}{2}^-$	$\frac{7}{2}^-$	1	1.003[+1]	2.859[+0]	6.003[−1]	2.010[+0]	2.451[−1]
		2	9.338[+0]	3.397[−1]	6.213[+0]	8.370[+0]	2.411[+0]
		3	1.022[+1]	4.041[+0]	1.727[+0]	3.103[+0]	2.703[+0]
$\frac{5}{2}^-$	$\frac{5}{2}^-$	1		−1.899[−1]	+2.232[−1]	+1.994[−2]	+3.988[−1]
				8.128[−1]	8.578[+0]	1.845[+0]	4.326[+0]
		2			−1.218[+0]	+1.526[+0]	−6.389[−1]
					3.509[+0]	4.307[+0]	3.748[+0]
$\frac{7}{2}^-$	$\frac{5}{2}^-$	1	+1.074[+0]	−2.104[+0]	−2.143[−1]	−4.249[−1]	+3.570[−1]
			1.021[+1]	1.048[+1]	3.324[+0]	2.922[+0]	2.107[+0]
		2	+6.673[−2]	−1.049[+0]	−2.146[+0]	+9.665[−1]	−1.015[+0]
			6.185[−1]	6.905[+0]	4.229[+0]	2.364[+0]	9.365[−1]
$\frac{7}{2}^-$	$\frac{7}{2}^-$	1		+2.227[−1]	+4.819[−2]	+3.505[−1]	+1.689[−1]
				1.128[+1]	8.886[−1]	6.509[+0]	2.962[+0]
		2			+3.863[−1]	+7.656[−1]	−9.442[−1]
					3.232[−1]	5.337[+0]	4.258[+0]
		3				−2.459[−1]	−1.484[+0]
						2.741[+0]	3.465[+0]

present calculations. Therefore mixing ratios were extracted for four transitions. The results are summarized in Table XI. Lifetime results for the low-lying ^{39}Ar levels are summarized in Table XII. These results, taken from the compilation of Ref. 6, are mainly from Sterrenburg *et al.*[25]

2. High-spin yrast spectra

The high-spin yrast states of ^{39}Ar were studied by Warburton *et al.*[23] and Keinonen *et al.*,[24] both of whom used γ-ray spectroscopy following fusion-evaporation reactions. Gamma-ray angular distributions and linear polarizations were determined in four reactions by Warburton *et al.* and level lifetimes were determined by Keinonen *et al.* Probable spin-parity assignments were made to the inferred levels based on the γ-ray data and on knowledge of the fusion-evaporation reaction mechanism. These probable assignments were $\frac{11}{2}^-$, $\frac{13}{2}^+$, $\frac{15}{2}^+$, and $\frac{17}{2}$ for the ^{39}Ar 2651-, 3992-, 4543-, and 5535-keV levels, respective-

TABLE XIV. Electromagnetic matrix elements, $M(\lambda)$, connecting $1\hbar\omega$ and $2\hbar\omega$ states of ^{39}Ar. The units and definition of $M(\lambda)$ are given in the text. The lowest (top) and next-to-lowest (bottom) allowed multipolarity, λ, is listed for each J_i^π, J_f^π combination.

			$M(\lambda)$				
			n_f				
J_f^π	J_i^π	n_i	1	2	3	4	5
$\frac{1}{2}^-$	$\frac{1}{2}^+$	1	1.396[−2]	8.204[−3]	2.954[−3]	5.676[−3]	2.361[−3]
		2	2.354[−2]	6.315[−3]	8.270[−3]	2.164[−3]	6.631[−3]
$\frac{3}{2}^-$	$\frac{1}{2}^+$	1	+8.321[−3]	+6.225[−3]	−1.118[−3]	−1.181[−2]	−3.187[−3]
			1.110[+0]	4.468[−3]	5.795[−2]	4.687[−1]	3.943[−2]
		2	+1.354[−2]	−1.953[−2]	−3.672[−3]	−3.206[−2]	−1.416[−2]
			9.862[−1]	8.997[−1]	6.023[−2]	4.823[−1]	2.832[−2]
		3	+4.929[−2]	−2.448[−2]	+1.905[−2]	+4.439[−2]	+2.029[−2]
			6.562[−1]	3.400[+0]	1.038[+0]	5.369[−1]	4.483[−1]
$\frac{5}{2}^-$	$\frac{1}{2}^+$	1	+8.409[−1]	+1.917[−1]	+5.602[−1]	−4.571[−2]	+2.836[−1]
			1.894[+0]	1.731[+0]	2.300[+0]	7.234[−1]	1.115[+0]
		2	+4.155[−1]	−9.091[−2]	−7.831[−2]	+1.623[−2]	+6.194[−1]
			6.746[+0]	1.304[+0]	1.580[+0]	5.755[−1]	2.069[−1]
$\frac{7}{2}^-$	$\frac{1}{2}^+$	1	1.808[+1]	3.102[+0]	5.667[−1]	3.691[+0]	1.397[+0]
		2	3.522[+1]	2.637[+0]	1.400[+0]	2.099[+0]	7.297[−2]
$\frac{1}{2}^-$	$\frac{3}{2}^+$	1	−2.865[−3]	−1.031[−3]	+1.725[−3]	+3.059[−3]	−2.486[−3]
			1.238[−1]	2.390[−2]	5.230[−2]	1.076[−1]	2.970[−2]
		2	+1.224[−2]	−5.584[−3]	−1.098[−3]	−3.923[−3]	−1.957[−2]
			1.150[−1]	2.812[−1]	4.358[−2]	8.033[−2]	7.014[−1]
		3	−7.883[−3]	−1.759[−3]	−1.218[−2]	−6.750[−3]	−2.242[−2]
			7.747[−2]	2.180[−1]	7.390[−2]	3.571[−2]	3.655[−1]
$\frac{3}{2}^-$	$\frac{3}{2}^+$	1	+4.849[−3]	+1.104[−2]	−3.952[−4]	+7.615[−3]	−8.366[−3]
			9.803[−2]	1.772[−1]	1.335[−2]	3.523[−2]	2.831[−2]
		2	−2.038[−4]	−5.455[−3]	−5.173[−4]	+6.080[−3]	+2.653[−2]
			1.448[+0]	5.782[−1]	5.486[−1]	1.026[−2]	3.572[−2]
		3	+1.795[+0]	−1.326[−1]	−3.306[−2]	+1.710[−1]	+2.392[−1]
			1.015[+0]	8.373[−1]	8.144[−2]	2.382[−1]	2.126[−1]
$\frac{5}{2}^-$	$\frac{3}{2}^+$	1	+3.430[−2]	−3.415[−3]	+1.016[−2]	+6.403[−3]	+1.172[−3]
			8.021[−1]	2.876[−1]	3.017[−1]	2.502[−2]	3.946[−1]
		2	−4.273[−2]	−1.499[−2]	−3.841[−2]	−1.712[−2]	+3.915[−3]
			5.768[−1]	3.472[−1]	1.247[−1]	2.253[−1]	2.701[−1]
		3	−1.540[−2]	−1.456[−2]	−2.333[−3]	−9.406[−3]	+1.964[−2]
			1.030[−1]	1.458[−1]	1.103[−1]	5.899[−2]	4.064[−2]
$\frac{7}{2}^-$	$\frac{3}{2}^+$	1	−3.590[+0]	+1.021[+0]	+3.028[−1]	−1.782[−1]	−1.627[−1]
			1.801[+1]	3.713[+0]	1.445[−1]	4.469[−1]	1.255[+0]
		2	−5.802[+0]	+6.661[−1]	−2.166[−1]	−1.288[−1]	−6.791[−1]
			1.322[+1]	3.830[+0]	8.176[−1]	1.876[+0]	2.098[+0]
		3	−9.373[+0]	+7.873[−1]	−8.237[−1]	+3.994[−1]	−1.054[+0]
			9.641[−2]	4.579[+0]	7.973[−1]	4.647[−1]	2.297[−1]
$\frac{3}{2}^-$	$\frac{5}{2}^+$	1	+2.014[−2]	+2.001[−2]	+2.473[−3]	+5.702[−4]	−4.472[−3]
			3.614[−2]	1.191[−1]	9.506[−2]	8.348[−2]	2.934[−2]
		2	−6.422[−5]	+1.539[−3]	+5.042[−3]	−1.204[−2]	−4.595[−3]
			3.648[−1]	4.861[−1]	1.529[−2]	3.099[−1]	3.183[−1]
$\frac{5}{2}^-$	$\frac{5}{2}^+$	1	+7.162[−2]	−2.170[−3]	+1.626[−2]	−1.017[−3]	+1.063[−2]
			1.187[−1]	1.023[−1]	3.811[−1]	1.711[−1]	5.577[−1]
		2	+1.025[−2]	+3.074[−3]	+1.190[−2]	−1.318[−2]	−2.145[−3]
			2.047[−1]	1.515[−1]	3.810[−2]	8.511[−2]	2.107[−1]
$\frac{7}{2}^-$	$\frac{5}{2}^+$	1	+2.455[−2]	−2.624[−2]	+7.236[−3]	−1.746[−2]	+6.938[−3]
			4.928[+0]	3.652[−1]	3.501[−1]	8.419[−1]	3.880[−1]
		2	+1.111[−2]	−8.908[−3]	+1.939[−2]	1.484[−2]	+3.034[−3]
			3.069[+0]	4.246[−1]	8.330[−1]	2.041[−1]	9.061[−2]

TABLE XIV. (*Continued*).

J_f^π	J_i^π	n_i	$M(\lambda)$ n_f 1	2	3	4	5
$\frac{3}{2}^-$	$\frac{7}{2}^+$	1	−3.218[−3]	+2.061[−1]	−1.634[−1]	+2.420[−1]	−8.963[−2]
			3.447[−2]	1.487[+0]	5.899[−1]	1.940[+0]	8.980[−1]
$\frac{5}{2}^-$	$\frac{7}{2}^+$	1	−2.035[−2]	+1.476[−3]	+5.811[−3]	−5.593[−3]	+2.667[−3]
			6.129[−1]	2.794[−1]	4.378[−1]	1.072[−1]	3.187[−1]
$\frac{7}{2}^-$	$\frac{7}{2}^+$	1	+1.490[−2]	+3.185[−2]	+3.153[−3]	+2.492[−4]	+7.775[−4]
			2.297[+0]	1.869[−1]	2.758[−1]	1.783[−1]	4.186[−1]

TABLE XV. Electromagnetic matrix elements, $M(\lambda)$, between $2\hbar\omega$ states of ^{39}Ar. The units and definition of $M(\lambda)$ are given in the text. When allowed, $M1$ (top) and $E2$ (bottom) matrix elements are given; otherwise the allowed $M(\lambda)$ is given.

J_f^π	J_i^π	n_i	$M(\lambda)$ n_f 1	2	3	4	5
$\frac{1}{2}^+$	$\frac{1}{2}^+$	1		6.983[−2]	1.480[−1]	9.786[−1]	6.829[−1]
		2			2.587[−1]	6.952[−1]	3.615[−1]
		3				5.436[−1]	1.042[+0]
		4					5.921[−1]
$\frac{1}{2}^+$	$\frac{5}{2}^+$	1	1.102[+1]	3.370[+0]	3.152[+0]	6.164[−1]	3.577[−1]
$\frac{3}{2}^+$	$\frac{1}{2}^+$	1	+1.146[−1]	+5.108[−1]	+9.473[−1]	−3.077[−1]	−3.231[−1]
			1.200[+1]	4.009[+0]	8.378[−1]	2.296[+0]	6.400[+0]
		2	−2.048[−1]	−4.762[−1]	+6.034[−1]	−1.112[−1]	−3.585[−1]
			5.369[+0]	5.739[−1]	1.197[+0]	1.070[+1]	3.799[+0]
		3	−3.994[−1]	+5.379[−2]	−6.630[−2]	+3.715[−1]	+6.759[−3]
			2.104[+0]	3.726[+0]	2.357[+0]	1.022[+0]	2.949[+0]
		4	+4.000[−1]	−3.344[−1]	+3.832[−1]	−6.484[−1]	6.558[−1]
			1.593[−1]	4.521[+0]	5.008[+0]	1.005[−1]	1.269[+0]
		5	+2.183[−1]	−1.008[+0]	+8.766[−1]	+8.360[−2]	+1.058[+0]
			1.511[+0]	1.950[+0]	2.017[+0]	2.577[+0]	3.832[−1]
$\frac{3}{2}^+$	$\frac{3}{2}^+$	1		+4.018[−1]	+4.366[−1]	−6.627[−2]	+6.747[−3]
				5.431[+0]	8.626[−2]	8.761[−1]	9.483[−1]
		2			+9.188[−1]	+7.258[−2]	+8.850[−1]
					4.447[−1]	1.201[+0]	1.994[+0]
		3				+3.721[−3]	+3.841[−1]
						5.611[+0]	3.003[+0]
		4					+3.551[−1]
							3.767[+0]
$\frac{3}{2}^+$	$\frac{5}{2}^+$	1	−4.433[−1]	+9.665[−1]	−8.676[−1]	−5.835[−1]	+6.887[−1]
			1.185[+1]	5.961[+0]	3.065[−1]	8.224[+0]	4.119[+0]
		2	−7.552[−1]	+1.314[−1]	−8.976[−2]	−3.651[−1]	+2.813[−1]
			3.295[+0]	4.308[+0]	6.024[+0]	4.772[+0]	2.197[+0]
		3	−9.359[−2]	+3.557[−1]	−5.712[−1]	−1.133[−1]	+5.973[−1]
			2.964[+0]	1.020[+1]	1.464[+0]	4.837[+0]	1.809[+0]
		4	−7.186[−1]	−4.254[−1]	+1.578[−1]	+3.273[−1]	−1.101[+0]
			5.433[+0]	4.113[+0]	5.867[+0]	4.775[−1]	5.103[−2]
		5	+6.496[−1]	−1.288[+0]	+5.473[−1]	+5.784[−1]	+1.328[−1]
			3.827[−1]	3.504[+0]	9.062[+0]	6.965[−2]	7.046[+0]
$\frac{3}{2}^+$	$\frac{7}{2}^+$	1	1.893[+1]	2.086[+0]	6.137[+0]	8.394[+0]	8.731[−1]

TABLE XV. (*Continued*).

					$M(\lambda)$ n_f		
J_f^π	J_i^π	n_i	1	2	3	4	5
$\frac{5}{2}^+$	$\frac{5}{2}^+$	1		3.950[−1]	+1.055[+0]	+3.086[−1]	+1.539[−2]
				8.024[+0]	1.440[+0]	3.354[+0]	2.661[+0]
		2			−3.878[−1]	−5.544[−1]	−1.089[+0]
					1.694[+0]	8.976[+0]	2.766[−2]
		3				−5.544[−1]	−1.219[+0]
						8.976[+0]	1.680[−1]
		4					+3.366[−1]
							1.370[+0]
$\frac{5}{2}^+$	$\frac{7}{2}^+$	1	+1.138[+0]	−5.607[−1]	+4.883[−1]	−6.060[−1]	+8.224[−1]
			2.643[−2]	9.658[+0]	2.597[+0]	2.486[+0]	8.842[+0]
		2	−7.737[−1]	+7.573[−2]	+1.404[−1]	+1.836[−1]	+1.504[−1]
			9.077[+0]	4.374[+0]	4.927[+0]	1.247[+0]	5.499[+0]
		3	−2.441[−1]	+7.611[−1]	+6.252[−1]	−3.681[−1]	−3.632[−1]
			5.550[+0]	5.583[+0]	6.711[+0]	1.756[+0]	9.979[−1]
$\frac{7}{2}^+$	$\frac{7}{2}^+$	1		+1.428[+0]	−8.688[−1]	−6.759[−2]	−2.494[−1]
				9.830[−1]	3.719[+0]	6.952[+0]	8.273[+0]

ly. A great deal of experimental data bearing on the fusion-evaporation reaction mechanism has been obtained in the ten years since these studies and the arguments used to make these probable spin-parity assignments can be considered to be much more compelling than was accepted at that time. Also, a subsequent ^{37}Cl(α,d)^{39}Ar experiment was performed[33] and $L=4$ and 6 transitions identified. (This is the origin of the 3440-keV state in Fig. 1, which we have speculated to be the $\frac{11}{2}^+$ state, this being the nearest $2\hbar\omega$ state with J in the required range.) The 5535-keV level was the level formed most intensely in the (α,d) reaction, which fixes it as even parity and led the authors to suggest $J=\frac{17}{2}$, in agreement with the suggestion of Ref. 23. Note that if the 5535-keV level has $J^\pi=\frac{17}{2}^+$, then the results of Refs. 23 and 24 combine to render the probable assignments to the other yrast levels as definite. In summary, the suggested spin-parity assignments for the 2651-, 3992-, 4543-, and 5535-keV levels are very probable indeed. Nevertheless, it is of interest to render these assignments as quantitative and rigorous as possible.

With this in mind, the data of Ref. 23 were reanalyzed. In this analysis the three members of the 4543 $\to$3992$\to$2651$\to$0 cascade were considered simultaneously. A fit was made to the angular distribution and linear polarization data and γ-ray multipolarities were restricted to have strengths smaller than the recommended upper limits (RUL's) of Endt.[21] No restrictions were placed on the alignment of the substates. However, to incorporate the fact that the side feeding of the levels is small (Ref. 23), the alignment of each level was required to be within 10% of that which would result from no side feeding at all. The results of this analysis, at the 0.1% confidence limit, are as follows: The 2651-keV level has $J^\pi=\frac{11}{2}^-$. The 4543$\to$3992 and 3992$\to$2651 transitions are of $J\pm1\to J$ character both with $|x(L+1/L)|<0.07$. The 3992- and 4543-keV levels have even parity. Thus the 3992-keV level has $J^\pi=\frac{9}{2}^+$ or $\frac{13}{2}^+$ and the 4443-keV level has $J^\pi=\frac{7}{2}^+$, $\frac{11}{2}^+$, or $\frac{15}{2}^+$. These are rigorous assignments. From them we evoke the reaction mechanism to choose the probable assignments indicated by the correspondence to the SDPF predictions in Fig. 1.

APPENDIX B: ELECTROMAGNETIC MATRIX ELEMENTS FOR ^{39}Ar

Matrix elements connecting the lower states of the model spaces $^{16}\text{O}(2s,1d)^{22}(1f,2p)^1$ and $^{16}\text{O}(2s,1d)^{21}(1f,2p)^2$—labeled as $1\hbar\omega$ and $2\hbar\omega$, respectively—are collected in Tables XIII, XIV, and XV. The matrix elements are described in Sec. II B. The units used here are $e\,\text{fm}^2$ and $\mu_N\,\text{fm}^{L-1}$ for EL and ML transitions, respectively. The sign convention is that of Rose and Brink (Ref. 15).

[1]F. C. Erné, Nucl. Phys. **84**, 91 (1966).
[2]S. Maripuu and G. A. Hokken, Nucl. Phys. **A141**, 481 (1970).
[3]D. H. Gloeckner, R. D. Lawson, and F. J. D. Serduke, Phys. Rev. C **7**, 1913 (1973).
[4]C. L. Woods, Nucl. Phys. **A451**, 413 (1986).
[5]E. K. Warburton, D. E. Alburger, J. A. Becker, B. A. Brown, and S. Raman, Phys. Rev. C **34**, 1031 (1986).
[6]P. M. Endt and C. van der Leun, Nucl. Phys. **A310**, 1 (1978).
[7]G. Wang, E. K. Warburton, and D. E. Alburger, Phys. Rev. C **35**, 2272 (1987), the preceding paper.
[8]B. H. Wildenthal, Prog. Part. Nucl. Phys. **11**, 5 (1984).
[9]B. H. Wildenthal, M. S. Curtin, and B. A. Brown, Phys. Rev. C **28**, 1343 (1983).
[10]A. G. M. van Hees and P. W. M. Glaudemans, Z. Phys. A **303**, 267 (1980).
[11]D. J. Millener and D. Kurath, Nucl. Phys. **A255**, 315 (1975).
[12]E. K. Warburton and J. B. Becker, Phys. Rev. C **35**, 1851 (1987).
[13]B. A. Brown, A. Etchegoyen, W. D. M. Rae, and N. S. Godwin, OXBASH, 1984 (unpublished).
[14]S. J. Skorka, J. Hertel, and T. Retz-Schmidt, Nucl. Data **A2**, 347 (1966).
[15]H. J. Rose and D. M. Brink, Rev. Mod. Phys. **39**, 306 (1967).
[16]B. A. Brown, in Proceedings of the International Nuclear Physics Conference, Harrogate, 1986.
[17]D. J. Millener, D. E. Alburger, E. K. Warburton, and D. H. Wilkinson, Phys. Rev. C **26**, 1167 (1982).
[18]B. A. Brown and B. H. Wildenthal, At. Data Nucl. Data Tables **33**, 347 (1985).
[19]E. K. Warburton, D. J. Millener, B. A. Brown, and J. A. Becker, Bull. Am. Phys. Soc. **31**, 1222 (1986), and unpublished.
[20]The meaning of weak, medium, and strong transition strengths is relative to the mean strength for a particular multipolarity. From Ref. 21, the logarithmic mean strengths for isospin allowed $E1$, $E2$, $E3$, $M1$, and $M2$ transitions in $A=4-44$ nuclear are about 5×10^{-3}, 4, 10, 0.1, and 0.3 W.u., respectively.
[21]P. M. Endt, At. Data Nucl. Data Tables **23**, 3 (1979).
[22]B. H. Wildenthal, privately circulated spectra predicted for $(2s,1d)$ nuclei by the USD interaction, 1983.
[23]E. K. Warburton, J. W. Olness, J. J. Kolata, and A. R. Poletti, Phys. Rev. C **13**, 1762 (1976).
[24]J. Keinonen, K. P. Lieb, H. P. Hellmeister, and F. J. Bergmeister, Z. Phys. A **282**, 227 (1977).
[25]W. A. Sterrenburg, G. Van Middlekoop, J. A. G. de Raedt, A. Holthuizen, and A. J. Rutten, Nucl. Phys. **A306**, 157 (1978).
[26]P. M. Endt, At. Data Nucl. Data Tables **19**, 23 (1977).
[27]C. Holbrow and B. Rosner, Nucl. Phys. **A91**, 551 (1967).
[28]W. Fitz, R. Jahr, and R. Santo, Nucl. Phys. **A114**, 392 (1968).
[29]S. Sen, C. L. Hollas, C. W. Biork, and P. J. Riley, Phys. Rev. C **5**, 1278 (1972).
[30]L. L. Lee and J. P. Schiffer, Phys. Rev. Lett. **12**, 108 (1964).
[31]I. S. Towner, E. K. Warburton, and G. T. Garvey, Ann. Phys. (N.Y.) **57**, 174 (1970).
[32]Analysis utilizing the Legendre polynomial coefficients rather than the angular distributions themselves will give closely the correct χ^2 minimum in an $x(L+1/L)$ vs χ^2 determination, but, because of the correlated uncertainties, may give somewhat inexact uncertainties for the extracted values of $x(L+1/L)$.
[33]H. Nann, W. S. Chien, A. Saha, and B. H. Wildenthal, Phys. Rev. C **15**, 1959 (1977).
[34]C. E. Thorn, J. W. Olness, E. K. Warburton, and S. Raman, Phys. Rev. C **30**, 1442 (1984).